ACS APPLIED MATERIALS & INTERFACES

www.acsami.org

Research Article

Organohydrogel Actuators with Adjustable Stimulus Responsiveness for On-Demand Morphing

Danyang Li, Xiaoxia Le,* Shuxin Wei, Hui Shang, Fuqing Shan, Guorong Gao, Jintao Yang,* and Tao Chen*

Cite This: *ACS Appl. Mater. Interfaces* 2023, 15, 16090−16096

Read Online

ACCESS | Metrics & More | Article Recommendations | Supporting Information

ABSTRACT: Hydrogel actuators showing shape morphing in response to external stimuli are of significant interest for their applications in soft robots, artificial muscles, etc. However, there is still a lack of hydrogel actuators with adjustable stimulus responsiveness for on-demand driving. In this study, an organohydrogel actuator was prepared by a two-step interpenetrating method, resulting in the coexistence of poly(*N*-isopropylacrylamide-*co*-4-(2-sulfoethyl)-1-(4-vinylbenzyl) pyridinium betaine) (p(NIPAM-SVBP)) hydrophilic networks and poly(lauryl methacrylate) (pLMA) hydrophobic networks with gradient distribution. In the initial state, the organohydrogel actuator can be driven globally under thermal stimulation. Owing to the unique alkali-chromic performance of SVBP, the organohydrogel actuator can be endowed with photothermal properties and actuate locally under the stimulus of NIR light. More importantly, the organohydrogel will return to the original colorless state after being treated with acid solution. Our work provides a new insight into designing and fabricating novel actuators with adjustable stimulus responsiveness for on-demand morphing.

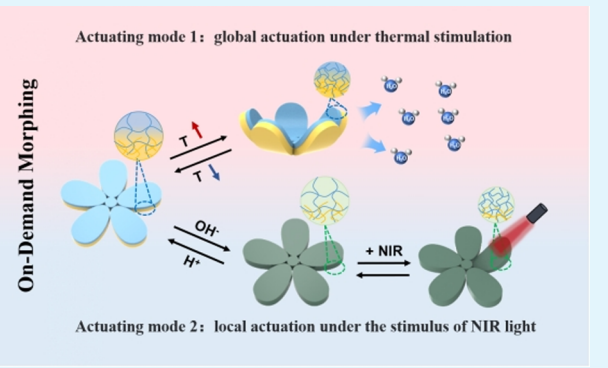

KEYWORDS: *stimulus responsive, zwitterionic polymer, organohydrogel actuator, on-demand morphing, anisotropic structure*

1. INTRODUCTION

As one of the most widely investigated smart soft matter, hydrogel actuators can convert external energy into kinetic energy, showing promising applications in fields of bionic robots,[1,2] artificial muscles,[3,4] drug delivery,[5,6] etc. Generally, the deformation behavior of hydrogel actuators is determined by two factors, intrinsic anisotropic structure and external stimulus.[7,8] Up to now, various asymmetric structures, including gradient structure, orientation structure, double-layer structure, and patterned structure, have been constructed.[9−12] As for the later, light, heat, magnetism, electricity, chemicals, etc. can all be employed to deform hydrogels through an elaborate design.[13−17]

Compared with other stimuli for hydrogel actuators, near-infrared (NIR) light possesses the characteristics of high accuracy, excellent penetration, and good manipulation.[18−20] In order to realize NIR-responsive actuation, photothermal conversion materials such as carbon materials, plasmons, and semiconductors are essential.[21−23] For example, Xue et al.[24] presented an NIR light-driven hydrogel with programmable shapes, which was prepared by free-radical copolymerization of *N*-isopropylacrylamide (NIPAM) and MXene nanomonomers. Xu's group[25] designed a MOF-loaded PNIPAM hydrogel that bonded with a poly(dimethylsiloxane) (PDMS) film for NIR light actuation, and programmable shapes can be tailored with the assistance of patterned PDMS films. Previously, our group has reported a biomimetic organohydrogel actuator containing rGO, which exhibits high actuation speed and synergistic fluorescence variation under the stimulus of NIR light.[26] However, once these hydrogel systems have been constructed, the corresponding stimulus-responsive modes are determined. In other words, hydrogel actuators with adjustable stimulus responsiveness for on-demand morphing are rare.

Herein, we adopted a two-step interpenetrating technique[27,28] to develop an anisotropic organohydrogel that shows stimulus responsiveness to temperature or NIR, which depends on whether it is treated with alkali solution. As shown in Scheme 1a, the poly(*N*-isopropylacrylamide-*co*-4-(2-sulfoethyl)-1-(4-vinylbenzyl) pyridinium betaine) (p(NIPAM-SVBP)) hydrogel was first prepared by free-radical copolymerization of the thermal-responsive monomer NIPAM and the alkali-chromic monomer SVBP. Then, the organohydrogel with a gradient structure was prepared by exposing oil precursor-

Received: January 19, 2023
Accepted: March 6, 2023
Published: March 16, 2023

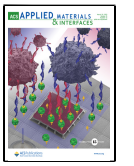

Scheme 1. Illustration of the Organohydrogel Actuator for On-Demand Morphing[a]

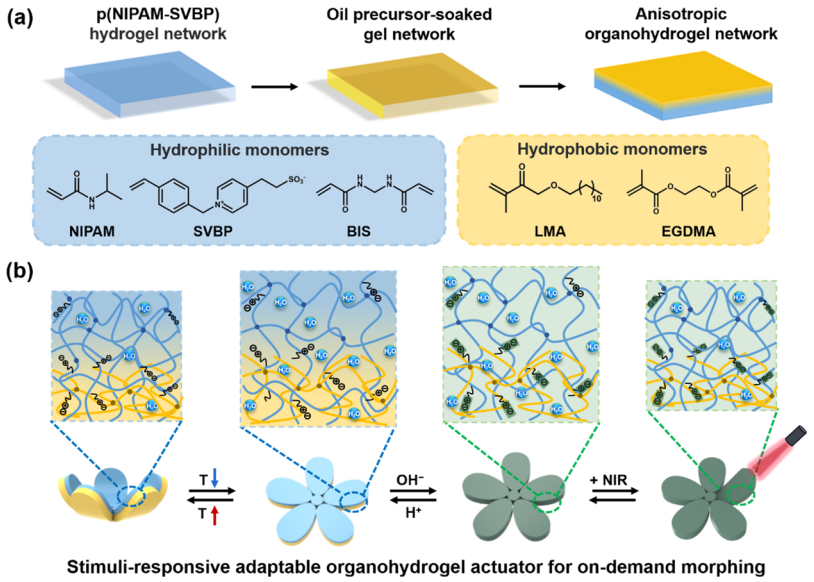

[a](a) Process of preparing the anisotropic organohydrogel via a two-step interpenetrating strategy. (b) Stimulus responsiveness of the organohydrogel actuator to temperature or NIR depends on whether it is treated by alkali solution or not.

soaked gel networks to UV light for a certain time. The obtained organohydrogel can be tailored into desired shapes such as a flower, which undergoes global deformation under the stimulus of homogeneous temperature (Scheme 1b). On the other hand, the alkali-chromic property of SVBP endows the organohydrogel with a dark green color when exposed to NaOH solution. Therefore, the organohydrogel actuator endowed with photothermal conversion performance can show localized deformation under NIR light. What is more, when the organohydrogel was treated with acid, the dark green color faded and made it only respond to the stimulus of temperature. This work proposes a new type of organohydrogel actuator with adjustable stimulus-responsive behavior, providing a new insight for the design of intelligent bionic actuators.

2. EXPERIMENTAL SECTION

2.1. Materials. 2-(4-Pyridyl)ethanesulfonic acid and NIPAM (≥98%) were purchased from TCI (Shanghai) Reagent Co. Ltd. 4-(Chloromethyl)styrene was bought from J&K Chemical Co. Ltd. Ammonium persulfate (APS, ≥98%), *N*,*N*′-methylene bis-(acrylamide) (BIS, ≥98%), ethylene glycol dimethacrylate (EGDMA, ≥98%), 2,2-diethoxyacetophenone (DEAP, ≥95%), and *N*,*N*,*N*′,*N*′-tetramethylethylenediamine (TEMED) were commercially provided by Aladdin Reagent Co. Ltd. Lauryl methacrylate (LMA) was purchased from Shanghai Macklin Biochemical Co. Ltd. Formamide, acetone, ethanol, sodium hydroxide (NaOH), and hydrogen chloride (HCl) were obtained from Sinopharm Chemical Reagent Co. Ltd. All reagents were used without any treatment or purification.

2.2. Synthesis of the Zwitterion Monomer SVBP. 2-(4-Pyridine) ethanesulfonic acid (18.72 g, 0.1 mol) and sodium hydroxide (4 g, 0.1 mol) were dissolved in formamide solution (150 mL) and stirred under the protection of N_2 for half an hour. Then, 4-chloromethyl styrene (15.2 g, 0.1 mol) was added into the above solution. After reaction for 72 h, the crude product can be obtained by pouring the reaction solution into acetone for precipitation. Finally, the white product can be obtained after washing with acetone for three times and drying.

2.3. Preparation of p(NIPAM-SVBP) Hydrogels. 0.75 g of NIPAM, 0.25 g of SVBP, 0.006 g of BIS (cross-linker), and 0.012 g of APS (initiator) were first dissolved in 10 mL of H_2O. After adding 20 μL of TEMED (accelerator), the mixture solution was poured into a homemade mold with two pieces of glasses sandwiched by a hollowed PDMS. After 24 h, the p(NIPAM-SVBP) hydrogel was put into acetone solution for dehydration.

2.4. Preparation of p(NIPAM-SVBP)/pLMA Organohydrogels. The organogel precursor solution was first prepared, which contains 40 mL of LMA, 20 mL of ethanol, 0.2 g of EGDMA, and 300 μL of DEAP. The dried p(NIPAM-SVBP) hydrogel was immersed in the above solution for 12 h. Then, the swollen hydrogel was exposed to UV light (365 nm, 50 W) for a certain time. Finally, the prepared organohydrogel was soaked in ethanol solution to remove the unreacted monomer and swelled to equilibrium in water.

2.5. Characterization. ^{1}H NMR spectra were obtained using a Bruker Avance III 400 MHz spectrometer. Fourier transform infrared (FTIR) spectra were obtained through an attenuated total reflection Fourier transformed infrared spectrometer (Thermo Scientific Nicolet 6700). The UV−vis absorption spectrum was recorded by a UV−vis spectrophotometer (TU-1810, Purkinje General Instrument Co. Ltd.). Field-emission scanning electron microscopy (SEM, S-4800, Hitachi) was used to observe the cross-section morphology of the organohydrogel and the alkali-treated organohydrogel. The contact angles between the two sides of the organohydrogel were measured by accurately controlling 3 μL of water droplets with an OCA 25 measuring machine at room temperature. ATR-FTIR spectra were recorded with an Agilent Scientific Cary 660+620 spectrometer. Rheological properties were performed on a stress-controlled rheometer (TADHR-2) with parallel plates (25 mm) in frequency scan mode (25 °C) at a constant shear strain of 1% and a frequency of 0.1−100 rad/s^{-1}. Microscopy images were obtained from an OLYMPUS BX51 polarizing microscope. The surface temperature and infrared images of the organohydrogel treated with different concentrations of sodium hydroxide were recorded by an Optris PI400.The data were analyzed by PI connect software. NIR light was provided by an NIR laser source (BWT Beijing, K808DAHFN-15.00 W, 808 nm), and the horizontal distance between the light and the samples was fixed at 7 cm.

https://doi.org/10.1021/acsami.3c00882
ACS Appl. Mater. Interfaces 2023, 15, 16090−16096

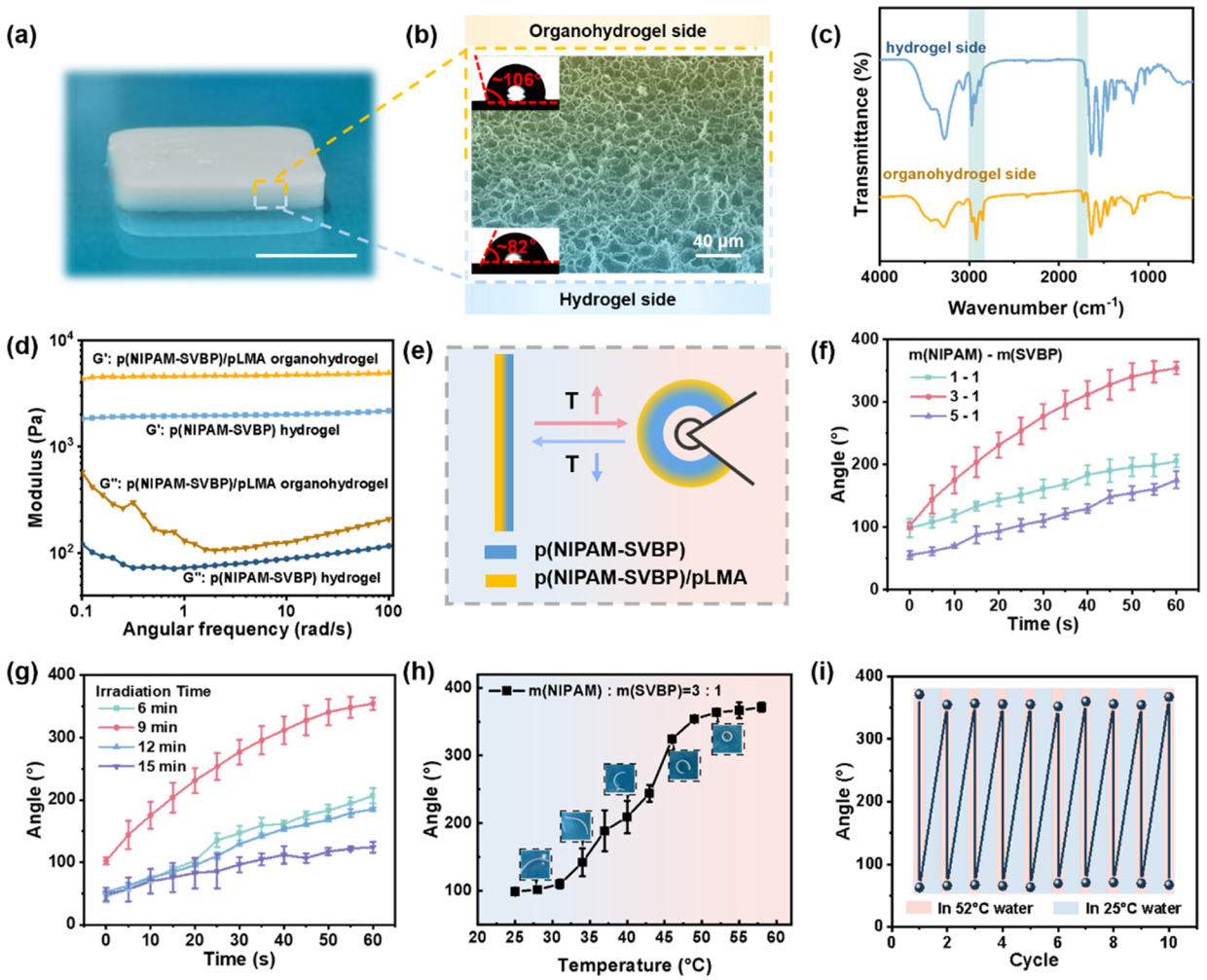

Figure 1. Actuation performance of the organohydrogel. (a) Photograph of the organohydrogel. The scale bar is 5 mm. (b) Cross-sectional SEM image of the p(NIPAM-SVBP)/pLMA organohydrogel and the contact angles for both sides. The scale bar is 40 μm. (c) ATR-IR spectra of the pure p(NIPAM-SVBP) hydrogel and p(NIPAM-SVBP)/pLMA organohydrogel. (d) G′ and G″ of the pure p(NIPAM-SVBP) hydrogel and p(NIPAM-SVBP)/pLMA organohydrogel. (e) Scheme of the strip organohydrogel actuation process. (f) Actuating degrees of various organohydrogels prepared by regulating the proportions of copolymerized monomers. (g) Actuating degrees of various organohydrogels prepared by tuning the time of UV irradiation (6, 9, 12, and 15 min). (h) Actuating degree of organohydrogels (9 min, the mass ratio of NIPAM and SVBP is 3:1) as a function of temperature. (i) Circular changes of bending angles for the organohydrogel actuator in water at 52 and 25 °C.

3. RESULTS AND DISCUSSION

3.1. Fabrication of p(NIPAM-SVBP)/pLMA Organohydrogels. The pH-responsive zwitterion monomer SVBP was first synthesized and characterized according to our previous work (Figures S1 and S2).[29] Then, the hydrogel network was fabricated via the copolymerization of NIPAM and SVBP in the presence of BIS as a cross-linker and APS as an initiator. After being dehydrated in acetone, the p(NIPAM-SVBP) hydrogel was swollen in an ethanol solution containing the hydrophobic monomer LMA, cross-linker EGDMA, and photoinitiator DEAP. Finally, the p(NIPAM-SVBP)/pLMA organohydrogel can be obtained after being irradiated by a UV lamp for a certain time. The anisotropic structure of organohydrogels can be adjusted by controlling the time of photopolymerization.

3.2. Anisotropic Structure Characterization and Actuation Performance of Organohydrogels. The construction of the anisotropic structure is the key for hydrogel actuators. Herein, the asymmetric organohydrogel was fabricated by regulating the introduction of the organogel network. As the hydrophobic monomer LMA was introduced into the p(NIPAM-SVBP) hydrogel during the process of photopolymerization, the macroscopic organohydrogel shows a gradient variation in transparency (Figure 1a). In order to ensure that UV light has no effect on SVBP, the samples of SVBP before and after UV light irradiation have been characterized by ^{1}H NMR, and the results showed that the structure of SVBP has no change under UV irradiation (FigureS3). Meanwhile, a porous structure with gradient sizes was observed by SEM (Figure 1b) and optical microscopy (Figure S4), in which the holes are denser on the organohydrogel side. Compared with the contact angle (CA) of the hydrogel side (82°), that of the other side was 106° due to the existence of the hydrophobic network, proving the asymmetric structure of the organohydrogel (Figure 1b). In addition, ATR-FTIR was conducted to characterize the chemical composition of both sides. As shown in Figure 1c, the emerging peak at 1729 cm^{-1} on the yellow line (organohydrogel side) is due to the presence of C═O groups in pLMA polymer chains, and the significant enhanced absorption peak at 2923.5 cm^{-1} is caused by the asymmetric

https://doi.org/10.1021/acsami.3c00882
ACS Appl. Mater. Interfaces 2023, 15, 16090−16096

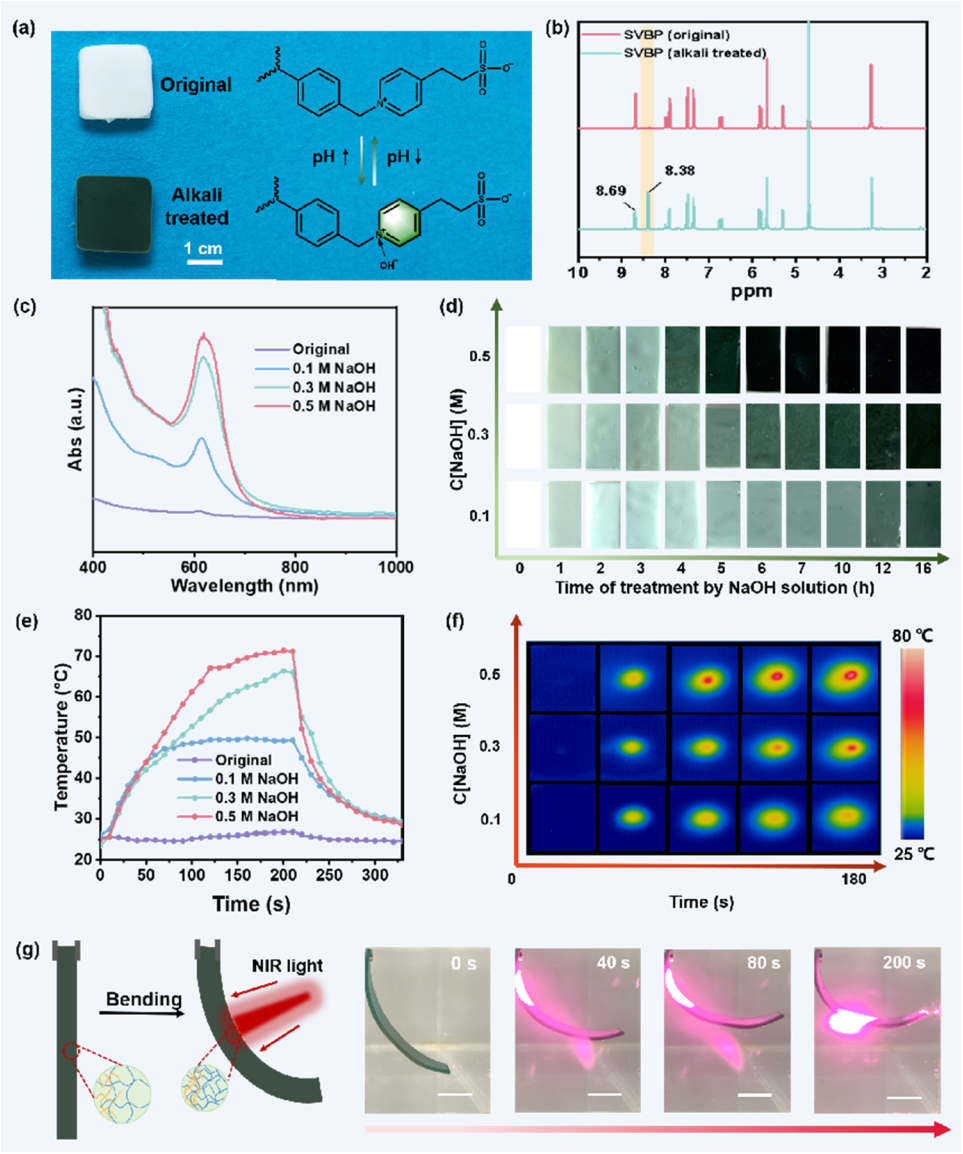

Figure 2. Alkali-chromic behavior of the organohydrogel actuator and NIR-responsive morphing. (a) Photos of the organohydrogel and structural changes of SVBP during the process of pH variation. (b) ^{1}H NMR spectra of pure SVBP aqueous solution and SVBP dissolved in alkali solution. (c) UV absorption spectra of p(NIPAM-SVBP)/pLMA organohydrogels treated with NaOH solution of different concentrations (0.1, 0.3, and 0.5 M). (d) Color block array of organohydrogels treated with different concentrations of NaOH solution (0.1, 0.3, and 0.5 M) over time. (e) Heating and cooling curves of organohydrogels obtained before and after soaking in alkali solution for 12 h and initial organohydrogels when turning on/off NIR light (808 nm, 5 W). (f) Pictures of different organohydrogels recorded by an infrared camera during the temperature-rise period (180 s). (g) Photothermal actuating process of an organohydrogel strip prepared by soaking in 0.3 M alkali solution for 12 h. The scale bar is 1 cm.

stretching of the $-CH_2-$ group.[30] What is more, rheological tests showed that the storage modulus (G') as well as loss modulus (G'') increase significantly after the introduction of the organogel network (Figure 1d). All the above results indicate the successful introduction of the PLMA network and construction of the anisotropic structure.

The actuation behavior of the hydrogel is ascribed to the nonuniform absorption or release of water in the hydrogel network.[31] The introduction of the pLMA network leads to the hydrophilic and hydrophobic difference between the two sides of the organohydrogel, resulting in different contraction rates of the pNIPAM network when stimulated by heat. Specifically, when temperature increases, the p(NIPAM-SVBP) hydrogel side exhibits faster contraction and thus it curves inward (Figure 1e). For optimal actuation performance, the ratio between NIPAM and SVBP was first investigated. Since SVBP is one kind of hydrophilic monomer,[32] on the one hand, the low critical solution temperature (LCST) of pNIPAM would be increased, and on the other hand, the introduction of the hydrophobic monomer LMA would be negatively affected. As depicted in Figure 1f, when the ratio of NIPAM and SVBP is 3:1, the organohydrogel actuator has both the maximum driving angle (360°) and fastest driving speed (60 s). Another crucial factor that affects actuating behavior is the time of photopolymerization, which determines the thickness of the organogel layer and affects the anisotropic structure of the organohydrogel. The actuating performance of organohydrogel actuators that were prepared by different photopolymerization times was measured (Figure 1g). Only when the irradiation time was 9 min, the prepared organohydrogel exhibited the

https://doi.org/10.1021/acsami.3c00882
ACS Appl. Mater. Interfaces 2023, 15, 16090−16096

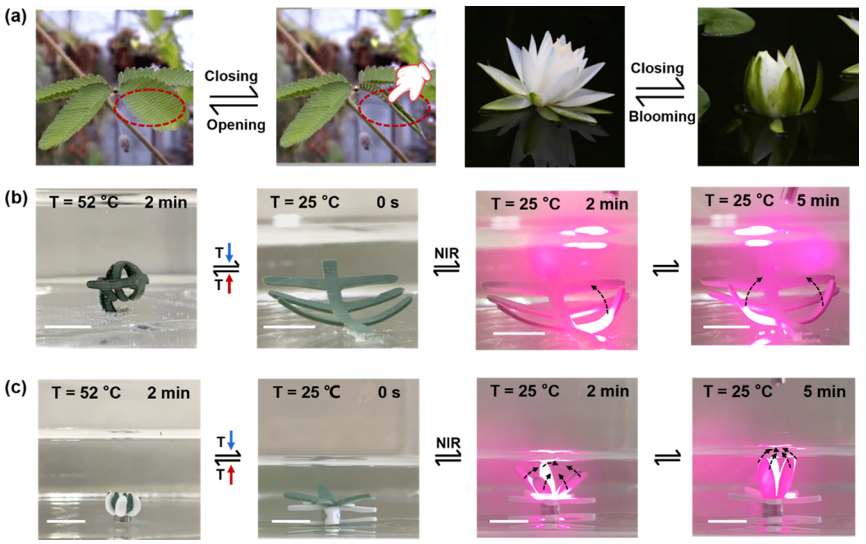

Figure 3. Demonstrations of organohydrogel actuators for on-demand morphing. (a) Photos of mimosa before and after touching by hand and lotus flower when blooming or closing. Deformations of mimosa-shaped (b) and lotus-shaped (c) organohydrogels under the stimulus of heat and NIR, respectively. The scale bar is 1 cm.

best actuating behavior. Therefore, the organohydrogel with a monomer ratio 3:1 and 9 min UV irradiation was selected as the target actuator. The organohydrogel actuator showed various bending angles in water with different temperatures, in which the straight strip of the organohydrogel reached a bending angle of 360° in 60 s when the temperature increased to 52 °C (Figure 1h). This bending and straightening process can be repeated at least 10 times without obvious changes by switching the temperature between 25 and 52 °C (Figure 1i). During the actuation cycles, the actuation time was set as 2 min and the recovery time was 40 min.

3.3. Alkali-Chromic Behavior of Organohydrogel Actuators and NIR-Responsive Morphing. As a unique zwitterionic monomer, SVBP shows reversible conformation change during the process of alkali treatment,[33] which is accompanied with color variation from white to dark green (Figures 2a and S5a). In order to understand the color change of SVBP, the ^{1}H NMR spectrum was used to study the conformational change of SVBP before and after alkali treatment. As illustrated in Figure 2b, an aromatic peak that blue-shifted from ≈8.69 to ≈8.38 ppm was observed, indicating the decrease in the π-electron cloud density due to the formation of conjugated styryl-pyridine structures. Meanwhile, compared with the original organohydrogel, a new characteristic absorption band at the range of 550−700 nm appears after treatment with NaOH solution, and the intensity of the absorption peak enhanced with the increase in NaOH concentration (Figures 2c and S5b). In addition, as more and more SVBP underwent conformation change, the green color of the organohydrogel gradually deepened with the increase in NaOH concentration as well as the extension of soaking time (Figure 2d). One interesting thing for our system is that the alkali-chromic performance of SVBP endowed the organohydrogel with great photothermal conversion efficiency. As depicted in Figure 2e, the temperature of the organohydrogels increased when irradiated by NIR light (808 nm, 5 W), and the higher NaOH concentration is, the faster the heating rate and the higher the final equilibrium temperature are. More obviously, the heating processes of round shape organohydrogels that are treated with different concentrations of NaOH solution are recorded by an infrared imager (Figures 2f and S6). Taking the concentration of NaOH solution and soaking time into consideration, the organohydrogel treated with NaOH solution (0.3 M) for 12 h shows the most suitable performance and was thus selected for further study. It is worth noting that though the pores of the organohydrogel treated with alkali solution became denser than those of the original organohydrogel (Figure S7), the driving performance was not affected at all (Figure S8). As illustrated in Figure 2g, a straight strip of the organohydrogel with one end fixed was exposed to NIR irradiation, leading to a quick bending caused by the differences in dehydration rates between the two sides. Furthermore, the discoloration behavior of the organohydrogel is completely reversible and can be repeated at least three times (Figure S9), indicating the great stability of our organohydrogel.

3.4. Organohydrogel Actuators for On-Demand Morphing. Animals in nature have their own day-night routines, so do plants. During a day, the sun rises and sets, and environmental factors such as light, temperature, humidity etc. change accordingly. In order to adapt to the above changes, plants would make corresponding changes in shapes, colors, and so on. For example, the leaves of mimosa close when disturbed, and the petals of lotus would open or close depending on the environment (Figure 3a). As a proof of concept, mimosa-shaped organohydrogels and lotus-shaped organohydrogels were studied as models. As demonstrated in Figure 3b and Movie S1, the whole "mimosa leaf" that is treated with alkali solution bent into a "ball" when the water temperature increases from 25 to 52 °C. Meanwhile, only individual blades bent due to the great space−time manipulability of NIR (Movie S2). As for "lotus", two layers of flower-shaped organohydrogels are bonded together, with the top layer treated with alkali solution and the bottom layer being original. When exposed to hot water (52 °C), the bilayer "lotus" both closed (Movie S3), while only the top layer closed when irradiated by NIR (Figure 3c and Movie S4). This phenomenon can be ascribed to the inhomogeneous structures and great photothermal effects of alkali-chromic SVBP. The organohydrogel actuator in this system has excellent

https://doi.org/10.1021/acsami.3c00882
ACS Appl. Mater. Interfaces 2023, 15, 16090−16096

adaptability to the stimulus sources, which provides a new idea for on-demand deformation of actuators and the development of new intelligent bionic devices.

4. CONCLUSIONS

In summary, an organohydrogel actuator with adjustable stimulus responsiveness for on-demand deformation was fabricated via a two-step interpenetrating technique. The organohydrogel was composed of the hydrophilic network that formed was by the copolymerization of the thermoresponsive monomer NIPAM and alkali-chromic monomer SVBP and the hydrophobic network that was formed by the photopolymerization of the hydrophobic monomer LMA. The anisotropic structure was successfully constructed by tuning the time of photopolymerization, leading to the hydrophilic and hydrophobic differences on both sides of the organohydrogel. As a result, the soft actuator can morph under the stimulus of heat, which was caused by the different dehydration rates. What is more, the zwitterionic monomer SVBP is able to change from colorless to dark green under alkaline conditions, endowing the organohydrogel with excellent photothermal properties. In consequence, the organohydrogel actuator can drive both as a whole by the thermal stimulation at the initial state and as a local drive by NIR light after alkali treatment. This system can inspire new ideas for the preparation of photothermal actuators and has potential application prospects in the field of intelligent software robots with adjustable stimulus responsiveness.

■ ASSOCIATED CONTENT

Supporting Information

The Supporting Information is available free of charge at https://pubs.acs.org/doi/10.1021/acsami.3c00882.

Synthetic route of SVBP; ^{1}H NMR (D_2O) spectrum of the zwitterion monomer SVBP; polarization microscopy schematic diagram of the p(NIPAM-SVBP)/pLMA organohydrogel cross-section; UV absorption spectra of SVBP in H_2O and in NaOH solution; schematic diagram of irradiation of p(NIPAM-SVBP)/pLMA organohydrogel samples with NIR light; final equilibrium temperatures of the p(NIPAM-SVBP)/pLMA organohydrogel that is treated with different concentrations of NaOH solution after irradiating with NIR; SEM of the section of the p(NIPAM-SVBP)/pLMA organohydrogel treated with 0.3 mol/L NaOH solution; actuating performance of the p(NIPAM-SVBP)/pLMA organohydrogel treated with 0.3 mol/L NaOH solution in 52 °C water; and cyclic discoloration behavior of the organohydrogel (PDF)

Deformations of mimosa-shaped organohydrogels under the stimulus of heat (Movie S1) (MP4)

Deformations of mimosa-shaped organohydrogels under the stimulus of NIR (Movie S2) (MP4)

Deformations of lotus-shaped organohydrogels under the stimulus of heat (Movie S3) (MP4)

Deformations of lotus-shaped organohydrogels under the stimulus of NIR (Movie S4) (MP4)

■ AUTHOR INFORMATION

Corresponding Authors

Xiaoxia Le − *Key Laboratory of Marine Materials and Related Technologies, Zhejiang Key Laboratory of Marine Materials and Protective Technologies, Ningbo Institute of Material Technology and Engineering, Chinese Academy of Sciences, Ningbo 315201, China; School of Chemical Sciences, University of Chinese Academy of Sciences, Beijing 100049, China;* orcid.org/0000-0003-3716-3076; Email: lexiaoxia@nimte.ac.cn

Jintao Yang − *College of Materials Science & Engineering, Zhejiang University of Technology, Hangzhou 310014, P. R. China;* orcid.org/0000-0002-3133-1246; Email: yangjt@zjut.edu.cn

Tao Chen − *Key Laboratory of Marine Materials and Related Technologies, Zhejiang Key Laboratory of Marine Materials and Protective Technologies, Ningbo Institute of Material Technology and Engineering, Chinese Academy of Sciences, Ningbo 315201, China; School of Chemical Sciences, University of Chinese Academy of Sciences, Beijing 100049, China;* orcid.org/0000-0001-9704-9545; Email: tao.chen@nimte.ac.cn

Authors

Danyang Li − *College of Materials Science & Engineering, Zhejiang University of Technology, Hangzhou 310014, P. R. China; Key Laboratory of Marine Materials and Related Technologies, Zhejiang Key Laboratory of Marine Materials and Protective Technologies, Ningbo Institute of Material Technology and Engineering, Chinese Academy of Sciences, Ningbo 315201, China*

Shuxin Wei − *Key Laboratory of Marine Materials and Related Technologies, Zhejiang Key Laboratory of Marine Materials and Protective Technologies, Ningbo Institute of Material Technology and Engineering, Chinese Academy of Sciences, Ningbo 315201, China; School of Chemical Sciences, University of Chinese Academy of Sciences, Beijing 100049, China*

Hui Shang − *Key Laboratory of Marine Materials and Related Technologies, Zhejiang Key Laboratory of Marine Materials and Protective Technologies, Ningbo Institute of Material Technology and Engineering, Chinese Academy of Sciences, Ningbo 315201, China; School of Chemical Sciences, University of Chinese Academy of Sciences, Beijing 100049, China*

Fuqing Shan − *Key Laboratory of Marine Materials and Related Technologies, Zhejiang Key Laboratory of Marine Materials and Protective Technologies, Ningbo Institute of Material Technology and Engineering, Chinese Academy of Sciences, Ningbo 315201, China*

Guorong Gao − *Key Laboratory of Marine Materials and Related Technologies, Zhejiang Key Laboratory of Marine Materials and Protective Technologies, Ningbo Institute of Material Technology and Engineering, Chinese Academy of Sciences, Ningbo 315201, China*

Complete contact information is available at: https://pubs.acs.org/10.1021/acsami.3c00882

Notes

The authors declare no competing financial interest.

■ ACKNOWLEDGMENTS

This work was supported by the National Key R&D Program of China (2022YFB3204300), the National Natural Science Foundation of China (52103246), the Zhejiang Provincial Natural Science Foundation of China (LQ22E030015), and

the Natural Science Foundation of Ningbo (20221JCGY010301).

REFERENCES

(1) Wei, S.; Lu, W.; Le, X.; Ma, C.; Lin, H.; Wu, B.; Zhang, J.; Theato, P.; Chen, T. Bioinspired Synergistic Fluorescence-Color-Switchable Polymeric Hydrogel Actuators. *Angew. Chem., Int. Ed.* **2019**, *58*, 16243−16251.
(2) Dong, Y.; Wang, J.; Guo, X.; Yang, S.; Ozen, M. O.; Chen, P.; Liu, X.; Du, W.; Xiao, F.; Demirci, U.; Liu, B. Multi-Stimuli-Responsive Programmable Biomimetic Actuator. *Nat. Commun.* **2019**, *10*, 4087.
(3) Oveissi, F.; Fletcher, D. F.; Dehghani, F.; Naficy, S. Tough Hydrogels for Soft Artificial Muscles. *Mater. Des.* **2021**, *203*, No. 109609.
(4) Jiang, Z.; Song, P. Strong and Fast Hydrogel Actuators. *Science* **2022**, *376*, 245.
(5) Ghawanmeh, A. A.; Ali, G. A. M.; Algarni, H.; Sarkar, S. M.; Chong, K. F. Graphene Oxide-Based Hydrogels as A Nanocarrier for Anticancer Drug Delivery. *Nano Res.* **2019**, *12*, 973−990.
(6) Yang, X.; Zhang, C.; Deng, D.; Gu, Y.; Wang, H.; Zhong, Q. Multiple Stimuli-Responsive MXene-Based Hydrogel as Intelligent Drug Delivery Carriers for Deep Chronic Wound Healing. *Small* **2022**, *18*, No. e2104368.
(7) Le, X.; Lu, W.; Zhang, J.; Chen, T. Recent Progress in Biomimetic Anisotropic Hydrogel Actuators. *Adv. Sci.* **2019**, *6*, No. 1801584.
(8) Ouyang, Y.; Huang, G.; Cui, J.; Zhu, H.; Yan, G.; Mei, Y. Advances and Challenges of Hydrogel Materials for Robotic and Sensing Applications. *Chem. Mater.* **2022**, *34*, 9307−9328.
(9) Ye, S.; Ma, W.; Fu, G. A Novel Nature-inspired Anisotropic Hydrogel with Programmable Shape Deformations. *Chem. Eng. J.* **2022**, *450*, No. 137908.
(10) Zhu, Q. L.; Dai, C. F.; Wagner, D.; Khoruzhenko, O.; Hong, W.; Breu, J.; Zheng, Q.; Wu, Z. L. Patterned Electrode Assisted One-Step Fabrication of Biomimetic Morphing Hydrogels with Sophisticated Anisotropic Structures. *Adv. Sci.* **2021**, *8*, No. e2102353.
(11) Li, Z.; Liu, P.; Ji, X.; Gong, J.; Hu, Y.; Wu, W.; Wang, X.; Peng, H. Q.; Kwok, R. T. K.; Lam, J. W. Y.; Lu, J.; Tang, B. Bioinspired Simultaneous Changes in Fluorescence Color, Brightness, and Shape of Hydrogels Enabled by AIEgens. *Adv. Mater.* **2020**, *32*, No. 1906493.
(12) Li, C. Y.; Hao, X. P.; Wu, Z. L.; Zheng, Q. Photolithographically Patterned Hydrogels with Programmed Deformations. *Chem. − Asian J.* **2019**, *14*, 94−104.
(13) Ma, C.; Lu, W.; Yang, X.; He, J.; Le, X.; Wang, L.; Zhang, J.; Serpe, M. J.; Huang, Y.; Chen, T. Bioinspired Anisotropic Hydrogel Actuators with On-Off Switchable and Color-Tunable Fluorescence Behaviors. *Adv. Funct. Mater.* **2018**, *28*, No. 1704568.
(14) Li, Y.; Liu, L.; Xu, H.; Cheng, Z.; Yan, J.; Xie, X. M. Biomimetic Gradient Hydrogel Actuators with Ultrafast Thermo-Responsiveness and High Strength. *ACS Appl. Mater. Interfaces* **2022**, *14*, 32541−32550.
(15) Zhang, D.; Zhang, J.; Jian, Y.; Wu, B.; Yan, H.; Lu, H.; Wei, S.; Wu, S.; Xue, Q.; Chen, T. Multi-Field Synergy Manipulating Soft Polymeric Hydrogel Transformers. *Adv. Intell. Syst.* **2021**, *3*, No. 2000208.
(16) Yu, Z.; Shang, J.; Shi, Q.; Xia, Y.; Zhai, D. H.; Wang, H.; Huang, Q.; Fukuda, T. Electrically Controlled Aquatic Soft Actuators with Desynchronized Actuation and Light-Mediated Reciprocal Locomotion. *ACS Appl. Mater. Interfaces* **2022**, *14*, 12936−12948.
(17) Paikar, A.; Novichkov, A. I.; Hanopolskyi, A. I.; Smaliak, V. A.; Sui, X.; Kampf, N.; Skorb, E. V.; Semenov, S. N. Spatiotemporal Regulation of Hydrogel Actuators by Autocatalytic Reaction Networks. *Adv. Mater.* **2022**, *34*, No. e2106816.
(18) Wei, X.; Chen, L.; Wang, Y.; Sun, Y.; Ma, C.; Yang, X.; Jiang, S.; Duan, G. An Electrospinning Anisotropic Hydrogel with Remotely-Controlled Photo-Responsive Deformation and Long-Range Navigation for Synergist Actuation. *Chem. Eng. J.* **2022**, *433*, No. 134258.
(19) Guo, Q.; Liu, Y.; Liu, J.; Wang, Y.; Cui, Q.; Song, P.; Zhang, X.; Zhang, C. Hierarchically Structured Hydrogel Actuator for Microplastic Pollutant Detection and Removal. *Chem. Mater.* **2022**, *34*, 5165−5175.
(20) Li, H.; Liang, Y.; Gao, G.; Wei, S.; Jian, Y.; Le, X.; Lu, W.; Liu, Q.; Zhang, J.; Chen, T. Asymmetric Bilayer CNTs-Elastomer/hydrogel Composite as Soft Actuators with Sensing Performance. *Chem. Eng. J.* **2021**, *415*, No. 128988.
(21) Zhao, Q.; Liang, Y.; Ren, L.; Yu, Z.; Zhang, Z.; Ren, L. Bionic Intelligent Hydrogel Actuators with Multimodal Deformation and Locomotion. *Nano Energy* **2018**, *51*, 621−631.
(22) Yu, W.; Deschaume, O.; Dedroog, L.; Garcia Abrego, C. J.; Zhang, P.; Wellens, J.; de Coene, Y.; Jooken, S.; Clays, K.; Thielemans, W. Light-Addressable Nanocomposite Hydrogels Allow Plasmonic Actuation and In Situ Temperature Monitoring in 3D Cell Matrices. *Adv. Funct. Mater.* **2022**, *32*, No. 2108234.
(23) Sun, Z.; Wei, C.; Liu, W.; Liu, H.; Liu, J.; Hao, R.; Huang, M.; He, S. Two-Dimensional MoO(2) Nanosheet Composite Hydrogels with High Transmittance and Excellent Photothermal Property for Near-Infrared Responsive Actuators and Microvalves. *ACS Appl. Mater. Interfaces* **2021**, *13*, 33404−33416.
(24) Xue, P.; Bisoyi, H. K.; Chen, Y.; Zeng, H.; Yang, J.; Yang, X.; Lv, P.; Zhang, X.; Priimagi, A.; Wang, L.; Xu, X.; Li, Q. Near-Infrared Light-Driven Shape-Morphing of Programmable Anisotropic Hydrogels Enable by MXene Nanosheets. *Angew. Chem., Int. Ed.* **2021**, *60*, 3390−3396.
(25) Zhang, X.; Xue, P.; Yang, X.; Valenzuela, C.; Chen, Y.; Lv, P.; Wang, Z.; Wang, L.; Xu, X. Near-Infrared Light-Driven Shape-Programmable Hydrogel Actuators Loaded with Metal-Organic Frameworks. *ACS Appl. Mater. Interfaces* **2022**, *14*, 11834−11841.
(26) Shang, H.; Le, X.; Si, M.; Wu, S.; Peng, Y.; Shan, F.; Wu, S.; Chen, T. Biomimetic Organohydrogel Actuator with High Response Speed and Synergistic Fluorescent Variation. *Chem. Eng. J.* **2022**, *429*, No. 132290.
(27) Gao, H.; Zhao, Z.; Cai, Y.; Zhou, J.; Hua, W.; Chen, L.; Wang, L.; Zhang, J.; Han, D.; Liu, M.; Jiang, L. Adaptive and Freeze-tolerant Heteronetwork Organohydrogels with Enhanced Mechanical Stability over A Wide Temperature Range. *Nat. Commun.* **2017**, *8*, 15911.
(28) Zhao, Z.; Li, C.; Dong, Z.; Yang, Y.; Zhang, L.; Zhuo, S.; Zhou, X.; Xu, Y.; Jiang, L.; Liu, M. Adaptive Superamphiphilic Organohydrogels with Reconfigurable Surface Topography for Programming Unidirectional Liquid Transport. *Adv. Funct. Mater.* **2019**, *29*, No. 1807858.
(29) Zhang, D.; Tang, Y.; Yang, J.; Gao, Y.; Ma, C.; Che, L.; Wang, J.; Wu, J.; Zheng, J. De Novo Design of Allochroic Zwitterions. *Mater. Today* **2022**, *60*, 17−30.
(30) Le, X.; Shang, H.; Wu, S.; Zhang, J.; Liu, M.; Zheng, Y.; Chen, T. Heterogeneous Fluorescent Organohydrogel Enables Dynamic Anti-Counterfeiting. *Adv. Funct. Mater.* **2021**, *31*, No. 2108365.
(31) Cheng, F. M.; Chen, H. X.; Li, H. D. Recent Progress on Hydrogel Actuators. *J. Mater. Chem. B* **2021**, *9*, 1762−1780.
(32) Meng, J.; Cao, Z.; Ni, L.; Zhang, Y.; Wang, X.; Zhang, X.; Liu, E. A Novel Salt-Responsive TFC RO Membrane Having Superior Antifouling and Easy-cleaning Properties. *J. Membr. Sci.* **2014**, *461*, 123−129.
(33) Zhang, D.; Tang, Y.; Zhang, C.; Huhe, F.; Wu, B.; Gong, X.; Chuang, S. S. C.; Zheng, J. Formulating Zwitterionic, Responsive Polymers for Designing Smart Soils. *Small* **2022**, *18*, No. e2203899.

https://doi.org/10.1021/acsami.3c00882
ACS Appl. Mater. Interfaces 2023, 15, 16090−16096